Journal of Applied Electrochemistry **29**: 533–539, 1999.

An integrated flow reactor-membrane filtration system for heterogeneous photocatalysis. Part I: Experiments and modelling of a batch-recirculated photoreactor

K. SOPAJAREE[1], S. A. QASIM[1], S. BASAK[2] and K. RAJESHWAR[2]*
[1]*Department of Civil and Environmental Engineering*
[2]*Department of Chemistry and Biochemistry, The University of Texas at Arlington, Arlington, Texas 76019, USA (*author for correspondence)*

Received 10 June 1998; accepted in revised form 17 November 1998

Key words: adsorption, dye photooxidation, titanium dioxide

Abstract

A two-part study was undertaken to examine the feasibility of combining a batch-recirculated photoreactor with a hollow-fibre membrane based ultrafiltration unit for heterogeneous photocatalysis applications. Methylene Blue (MB) and titanium dioxide (Degussa, P-25) were used as the test substrate and photocatalyst respectively for this study. This paper, which forms Part I of this study, describes the influence of MB concentration, recirculation flow rate, TiO_2 dose, solution volume in the reservoir and solution pH on the photocatalytic reaction rate. The dark adsorption of MB on the TiO_2 particle surface was also analysed. The combination of the reservoir and the annular reaction vessel could be modelled as a continuous flow stirred tank in series with a plug-flow reactor. This model predicts that the reaction rate should increase with a decrease of solution volume in the reservoir, both in the low and high substrate concentration regimes of the Langmuir–Hinshelwood kinetics formalism. This prediction was borne out by the experimental data for the low concentration regime. Part II of this series will describe experiments and modelling of the UF unit, and the operation of the combined system, respectively.

1. Introduction

Heterogeneous photocatalysis, based largely on the use of TiO_2 as a photocatalyst, has proven to be an effective method for the treatment of environmental pollutants [1–3]. One of the challenges in further development of this technology for water-borne pollutants, is an effective means of separating the photocatalyst particles from the treated water stream and recycling them into the photoreactor [4, 5]. Although this process step is obviated by the use of an immobilized photocatalyst film, slurry-based photoreactors do have attractive features; for example, higher photocatalyst surface area, lower susceptibility to surface poisoning/passivation effects etc. Thus this study explores the feasibility of combining a batch-recirculated photoreactor with a hollow-fibre membrane ultrafiltration (UF) unit for heterogeneous photocatalysis applications.

Figure 1 contains a schematic diagram of the integrated system. In a typical sequence, after the flow stream is treated in the photoreactor for a predetermined time, it is routed into the membrane UF unit. The retentate from the latter (consisting of a photocatalyst 'cake') is redispersed into a fresh stream in the reservoir for a further treatment cycle. Up to ten such repeat cycles were employed in the present study.

As a prelude to studying the variables associated with the UF process, and the combined approach, Part I of this series of papers describes experiments and analyses on the flow-through (recirculated) batch photoreactor. Part II will describe experiments and modelling of the UF process along with the combined approach. Methylene Blue (MB) was used as a test pollutant for this study and TiO_2 was used as the photocatalyst.

2. Experimental details

As Figure 1 illustrates, the photoreactor consists of two parts: reaction vessel and reservoir tank. The reaction

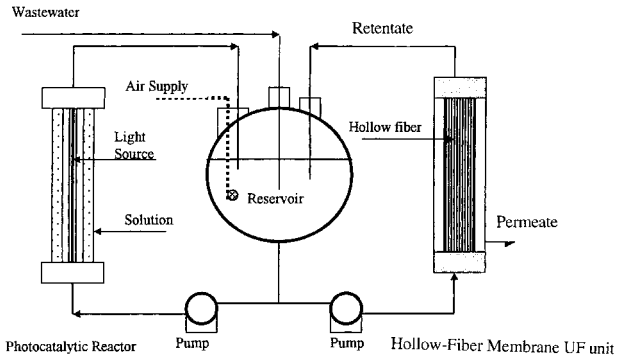

Fig. 1. Schematic diagram of the integrated photoreactor-membrane UF system.

vessel has an annular shape with an inner (quartz tube) diameter of 35 mm and an outer (Pyrex tube) diameter of 54 mm. It has a volume of 350 mL. The Teflon tube connects the reaction vessel to a reservoir and a variable-speed magnetically driven centrifugal pump. An air diffuser was connected to the air supply line for supplying air and for solution agitation. The latter served to maintain the TiO_2 particles in suspension in the reservoir tank. A nominal air flow rate of 1 dm^3 min^{-1} was employed. Temperature control in the reservoir tank was provided by circulating cold water around it. The ultraviolet (u.v.) light source was placed in the inner quartz tube to provide illumination to the photoreactor. All solutions were prepared to 1 dm^3 volume unless otherwise noted.

The incident light intensity (not adjusted for scattering by the TiO_2 particles or by refraction at the reactor wall) was measured by a radiometer/photometer (Biospherical Instrument, San Diego, model QSL-100). A 15 W NEC blacklight was used as the light source. The light intensity was about 0.183 mE s^{-1} m^{-2} (mE denotes 10^{-3} einstein).

The experimental variables for this study included initial MB concentration, recirculation flow rate, TiO_2 dose, solution volume in the reservoir and pH. Prior to each run, the prepared MB solutions were circulated in the photoreactor and reservoir tank for 5 min. Then, requisite amounts of TiO_2 particles were added to the reservoir tank. During the experiment, tap water was circulated through the outer shell of the reservoir in order to maintain a constant temperature in the system (nominally 22 $\pm$ 2 °C).

The adsorption of MB on the TiO_2 particle surface was studied by equilibrating MB solutions of varying concentration with the TiO_2 slurry in the dark. The solutions were then periodically sampled by withdrawing aliquots and centrifuging the latter at high speed using an Adams analytical centrifuge to remove the suspended TiO_2 particles. The MB concentrations were spectrophotometrically determined [6, 7] at an analytical wavelength of 660 nm using a Hewlett-Packard (HP) model 8452A diode array u.v.–vis. spectrophotometer fitted with a HP model 300 desktop computer. The progress of the photocatalysis reaction was similarly monitored.

Methylene Blue (MB) was from Aldrich and was used without further purification. The TiO_2 samples were from Degussa (P-25) and had a nominal surface area of 60 m^2 g^{-1}. Solutions were made up with doubly distilled water, and all experiments pertain to the laboratory ambient temperature.

3. Results and discussion

3.1. *Adsorption of MB on the TiO_2 particle surface in the dark*

Figure 2(a) illustrates how the amount of MB adsorbed onto TiO_2 varies with time and the initial level of MB in the solution. The TiO_2 dose in the latter was kept constant at 1 g dm^{-3}. Adsorption is essentially complete after about 15 min. These data can be analysed via the Langmuir adsorption isotherm model expressed in the reciprocal format:

$$\frac{1}{[\mathrm{MB}]_{\mathrm{ads}}} = \frac{1}{k_2} + \frac{1}{k_1 k_2} \times \frac{1}{[\mathrm{MB}]} \tag{1}$$

In Equation 1, $[MB]_{ads}$ is the adsorbed MB concentration, [MB] is the initial MB level in solution, and k_1 and k_2 are parameters related to the adsorption affinity and saturation coverage, respectively. Figure 2(b) contains such a plot for the data in Figure 2(a). From regression analysis, k_1 and k_2 can be determined to be 0.162 dm^3 mg^{-1} and 23.09 mg dm^{-3}, respectively.

These results may be compared with those obtained by a previous author [6] for a batch recirculation photoreactor in which Degussa (P-25) TiO_2 particles were attached in a thin film to the inner wall of borosilicate glass tubing wound in a spiral [6]. Values for k_1 and k_2 of 0.0934 dm^3 mg^{-1} and 1.621 mg dm^{-3} were quoted in this study. The higher values observed for these parameters in our study underline the key advantage in the use of slurry suspensions vis-à-vis thin films that was noted in an introductory paragraph; viz., namely of higher surface area for the photocatalyst.

3.2. *Photocatalytic oxidation of MB in the batch recirculation photoreactor*

Figure 3(a) contains plots of the MB concentration against time under blacklight illumination of solutions

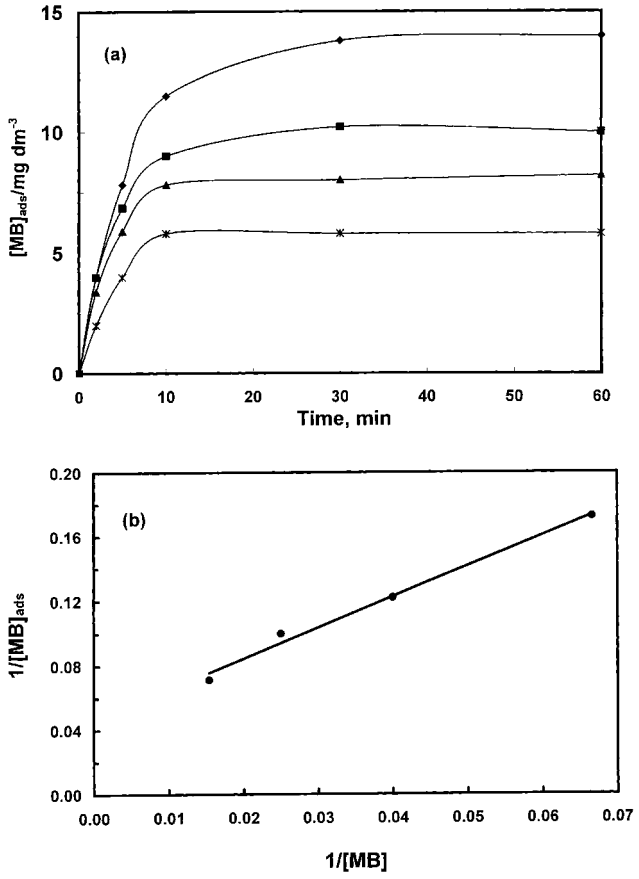

Fig. 2. (a) Variation of the amount of MB adsorbed on the TiO_2 particle surface with time. The initial MB concentration (mg dm^{-3}) is the parameter, and is 65, 40, 25 and 15 from top to bottom. TiO_2 dose 1 g dm^{-3}. (b) Reciprocal plot of $1/[MB]_{ads}$ against 1/[MB] using the data in Figure 2(a). Solid line: least-squares fit of data points.

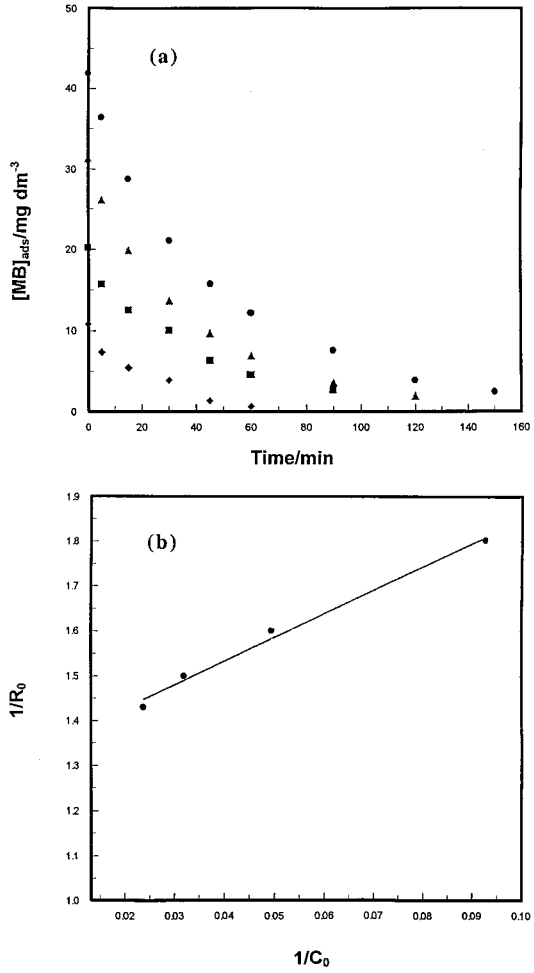

Fig. 3. (a) Variation of MB concentration with time during blacklight illumination of a 1 g dm^{-3} TiO_2 slurry suspension. The parameter is the initial MB concentration (mg dm^{-3}) that was varied: (◆) 11, (■) 20, (▲) 31 and (●) 42. The recirculation flow-rate was 1.87 dm^3 min^{-1}. (b) Reciprocal plot of $1/R_o$ (R_o = initial rate) against $1/C_o$ (C_o is the initial concentration of MB) of the data in Figure 3. Solid line: least-squares fit of data points.

with 1 g dm^{-3} TiO_2 dose and a flow rate of 1.873 dm^3 min^{-1}. These solutions were preequilibrated in the dark for about 15 min prior to initiation of the photocatalysis reaction. These data can be analysed within the framework of the Langmuir–Hinshelwood kinetics model [2, 3] expressed in reciprocal format:

$$\frac{1}{R_o} = \frac{1}{R_s} + \frac{1}{k_1 R_s} \times \frac{1}{C_o} \qquad (2)$$

In Equation 2, R_o is the initial reaction rate (that can be estimated from the initial slopes of the plots in Figure 3(a), R_s is the saturation rate (i.e., at high substrate levels when the reaction tends to zero-order kinetics behavior, see below) and C_o is the initial MB concentration. The parameter k_1 was defined earlier. A reciprocal plot (Figure 3(b)) thus would yield k_1 and R_s from the slope and intercept, respectively. Regression analyses of the data in Figure 3(b) yielded values for k_1 and R_s of 0.254 dm^3 mg^{-1} and 0.756 mg dm^{-3} min^{-1}.

It is interesting to note that the values obtained for k_1 are different in the dark and light conditions of the TiO_2/MB interface, the k_1 value being about 60% higher in the latter case. Whether this reflects the fact that the adsorption tendency of MB is enhanced by irradiation of the photocatalyst surface requires further study. This issue has also been addressed by other authors [8]. On the other hand, a previous study on TiO_2 *films* [6] reports good agreement between the k_1 values in the two cases, again underlining the fact that the slurry and thin film photocatalyst configurations perhaps are not strictly comparable.

3.3. *Influence of various experimental variables on the photocatalytic oxidation rate*

At low concentrations of MB (~10 mg dm^{-3} or lower), the Langmuir–Hinshelwood model predicts simple first-order kinetics behaviour:

$$R_o \simeq k_1 R_s C_o = k C_o \quad (3)$$

In this scenario, semilog plots of C/C_o against time should be linear, the slopes of which would yield estimates of k. Thus the apparent first-order rate constant, k (min^{-1}) can be used as a comparative measure to assess the influence of the various experimental variables on the overall reaction rate. Four such variables, namely the recirculation flow rate, TiO_2 dose, solution volume in the reservoir and solution pH were investigated. The corresponding results are presented in Figures 4–8 and in Tables 1–3, respectively. In some cases, semilog plots are also shown to underline the extent of adherence to the first-order kinetics limiting condition.

These experiments reveal that the recirculation flow rate has a weak, albeit, systematic influence on the reaction rate (Figure 4 and Table 1). The rather noticeable 'jump' in the rate constant at a flow rate higher than 4.8 dm^3 min^{-1} (Table 1) is probably caused by the onset of turbulent flow within the photoreactor. The TiO_2 dose data (Figure 5 and Table 2) merit little discussion. As expected, the photocatalysis reaction rate decreases with decreasing TiO_2 dose. It is possible that doses higher than 2 g dm^{-3} will exert a progressively diminishing influence (on the reaction rate) although the use of such doses was avoided in this study because of concerns with excessive light scattering by the suspended particles.

Figure 6 and Table 3 contain data illustrating the influence of solution volume on the reaction rate. The rate increases with decreasing solution volume. This trend is in good accord with the prediction from the photoreactor model presented in the next section. The effect of solution pH on the reaction rate is addressed in the data in Figures 7 and 8. The pH was adjusted in the range from 5 to 12 by adding a buffer consisting of 0.2 mol dm^{-3} anhydrous boric acid, 0.05 mol dm^{-3} citric acid monohydrate, and 0.1 mol dm^{-3} Na_3PO_4. 12 H_2O. The photocatalysis proceeds faster with increasing pH (Figure 7), and the rate constant shows an appreciable jump between 7 and 9.

The trends in Figures 7 and 8 are best rationalized by considering the hydroxyl ion concentration at the TiO_2 particle/solution interface with increasing pH. An increase in the concentration of this specie promotes the

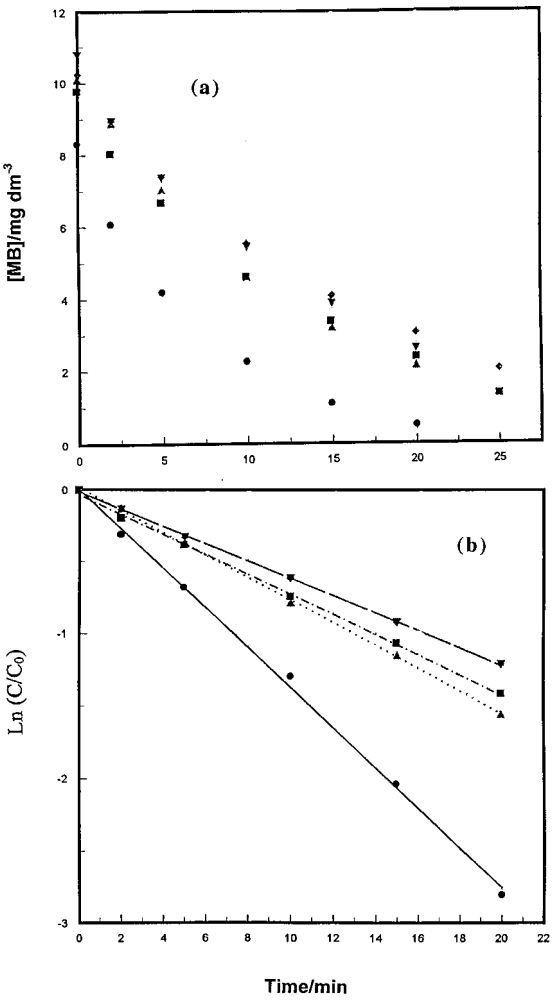

Fig. 4. (a) Variation of MB concentration with time during blacklight illumination of a 1 g dm^{-3} TiO_2 slurry suspension. The parameter is the recirculation flow-rate (dm^3 min^{-1}) that was varied (▼) 1.87, (◆) 2.62, (■) 3.24, (▲) 4.80 and (●) 5.05. Initial MB concentration in these experiments was 10 mg dm^{-3}. (b) First-order kinetics plots of the data in Figure 4(a). Lines are least-squares fits of the data points.

photocatalytic reaction by facilitating the generation of $^{\cdot}OH$ at the TiO_2 particle/solution interface:

$$TiO_2 \xrightarrow{h\nu} e^- + h^+ \quad (4a)$$

$$OH^- + h^+ \rightarrow OH^{\cdot} \quad (4b)$$

Hydroxyl radicals have been implicated in the photocatalytic oxidation of many organic substrates [2].

3.4. *Photoreactor model*

The photoreactor, comprising of the reservoir and the reaction vessel (Figure 1), can be modelled as a continuous flow stirred tank (CFST)-plug flow reactor (PFR)

combination [9] (Figure 9(a)). Consideration of the mass-balance in the reservoir yields:

$$V_1 \frac{dC_2}{dt} = QC_1 - QC_2 \quad (5)$$

In Equation 5, C_2 is the concentration of MB in the reservoir, V_1 is the reservoir volume, Q is the volumetric flow rate and C_1 is the inlet concentration of MB into the reservoir.

The annular reaction vessel can be modelled as a PFR. It is assumed that mixing occurs only in the lateral direction (around the tube perimeter, but not along its length). Figure 9(b) contains a cross-sectional diagram of the annular reaction vessel. The corresponding equation is

$$\int_{C_1}^{C_2} \frac{dC}{R} = -\int_{o}^{V_2} \frac{dV}{Q} \quad (6)$$

Table 1. Dependence of the pseudo first-order rate constant on the recirculation flow rate in the photoreactor*

Recirculation rate /dm^3 min^{-1}	k /min^{-1}
5.05	0.1375
4.80	0.0770
3.24	0.0720
2.62	0.0710
1.87	0.0610

* From the data in Figure 4.

Table 2. Dependence of the pseudo first-order rate constant, k, on TiO_2 dose*

TiO_2 dose /g dm^{-3}	k /min^{-1}
2.0	0.0219
1.5	0.0159
1.0	0.0100
0.5	0.0081

* From the data in Figure 5.

Table 3. Dependence of the pseudo first-order rate constant, k, on the solution volume in the reservoir*

Volume /dm^3	k /min^{-1}
1.0	0.0775
0.9	0.1026
0.8	0.1028
0.7	0.1258
0.6	0.2234

* From the data in Figure 6.

In Equation 6, dC is the change in MB concentration after passage through the reaction vessel, R is the photocatalytic reaction rate (expressed on unit volume basis) and V_2 is the reaction vessel volume.

This equation can be combined with the CFST expression (Equation 5) and the limiting first-order kinetics (cf. Equation 3) embodied within the Langmuir–Hinshelwood model framework:

$$R = kC \quad (7)$$

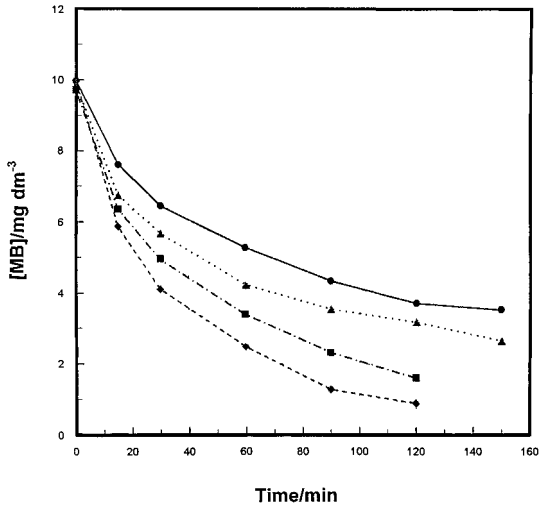

Fig. 5. Variation of MB concentration with time (as in Figure 4(a)) but with the TiO_2 dose (g dm^{-3}) as a parameter: (●) 0.5, (▲) 1.0, (■) 1.5 and (◆) 2.0. Recirculation flow-rate and initial MB concentration in these experiments: 1.87 dm^3 min^{-1} and 10 mg dm^{-3}, respectively.

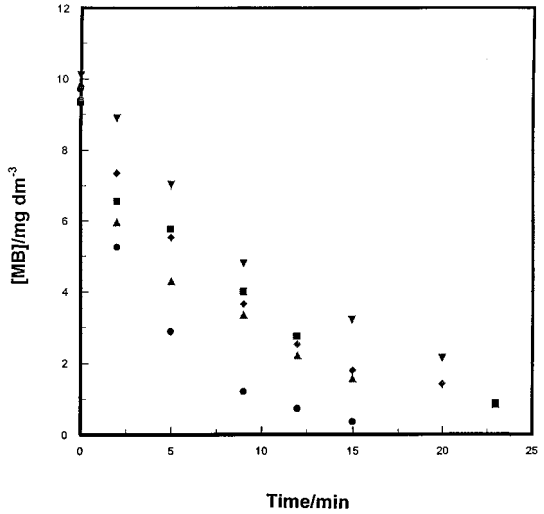

Fig. 6. As in Figure 4(a) but with the solution volume (dm^3) in the reservoir (see Figure 1) as a parameter: (●) 0.6, (▲) 0.7, (■) 0.8, (◆) 0.9 and (▼) 1.0. TiO_2 dose 1 g dm^{-3}; recirculation flow-rate 4.8 dm^3 min^{-1}; initial MB concentration 10 mg dm^{-3}.

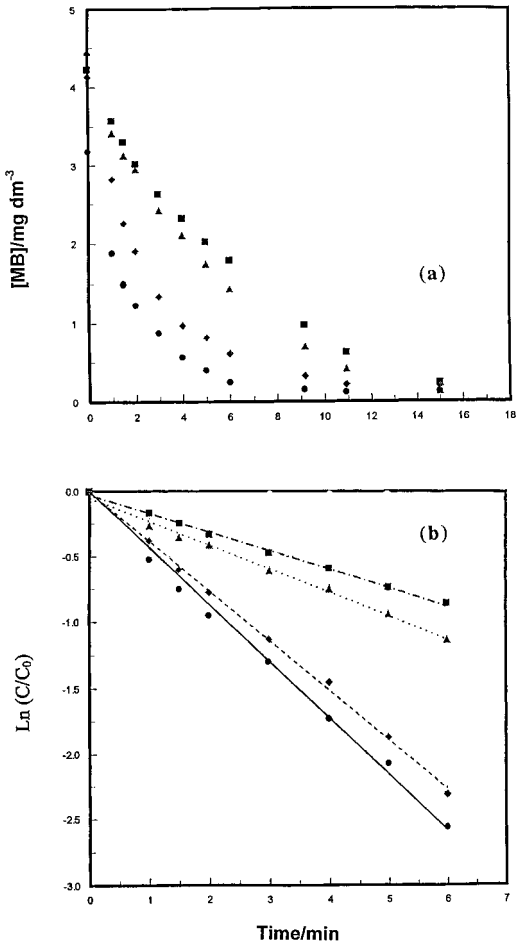

Fig. 7. (a) As in Figure 4(a) but with the solution pH as parameter: (■) 5, (▲) 7, (◆) 9 and (●) 12. TiO_2 dose 0.5 g dm^{-3}; recirculation flow rate 1.87 dm^3 min^{-1}; initial MB concentration 5 mg dm^{-3}. (b) First-order kinetics plots of the data in Figure 7(a). Lines are least-squares fits of data points.

to yield an expression for the overall CFST–PFR combination as applied to photocatalysis:

$$-\frac{dC_2}{dt} = \frac{1}{\Theta_1}[1 - \exp(-k\Theta_2)]C_2 \equiv k_{app}C_2 \qquad (8)$$

In Equation 8, $\Theta_1 = V_1/Q$ and $\Theta_2 = V_2/Q$, these parameters being the space times in the CFST and PFR, respectively. Equation 8 predicts that k_{app} will increase if Θ_2 increases or Θ_1 decreases. Since V_2 is constant (0.350 dm^3 in the present study), the only factor that modulates the reaction rate is Θ_1. This then explains the trends in Figure 6 and Table 3 above. As V_1 is decreased (at fixed Q), Θ_1 decreases and the reaction rate increases concomitantly.

In summation, Part I of this study has addressed the variables that influence the photocatalysis reaction rate

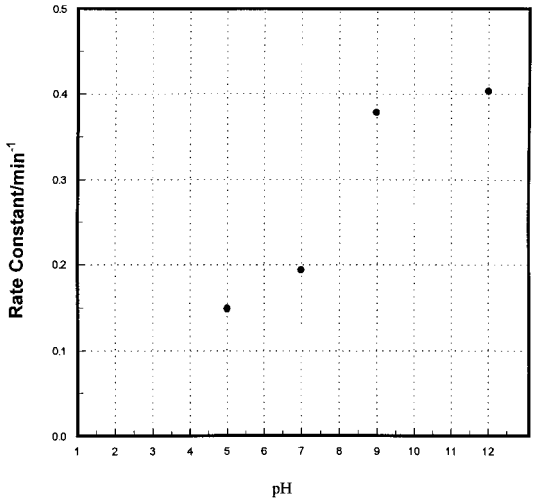

Fig. 8. Variation of the first-order rate constants (obtained from the slopes of the lines in Figure 7(b)) with solution pH.

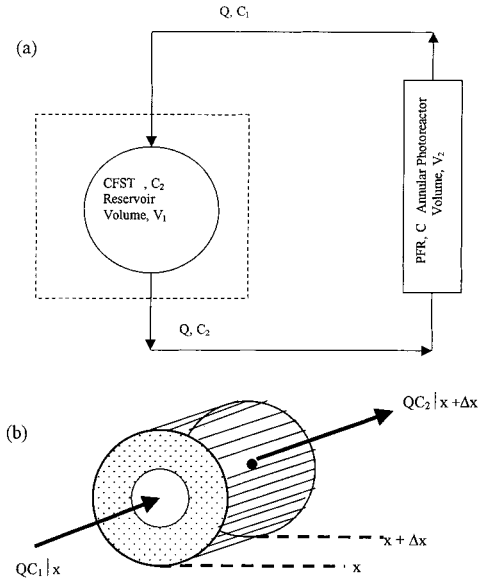

Fig. 9. (a) Schematic diagram of the photoreactor used in this study (cf. Figure 1) in terms of the reactor model designations and the corresponding parameters. Refer to text for notation of symbols. (b) Cross-section of the annular reaction vessel modelled as a plug-flow reactor (PFR).

in a batch-recirculated photoreactor consisting of a reservoir and an annular reaction vessel. The latter can be modeled as a CFST and a PFR, respectively. Part II of this series of papers [10] will describe experiments and modeling of a hollow-fibre membrane UF assembly, and the data from the integrated system.

Acknowledgements

This study was funded in part by a subcontract from the National Renewable Energy Laboratory (subcontract XCK 0-5-14318-03). K.S. thanks the Royal Government of Thailand for a Faculty Development Grant to undertake this dissertation research at the University of Texas at Arlington. We thank Ms G. Madden for assistance in the preparation of this manuscript and the two reviewers for positive criticisms of an earlier manuscript version.

References

1. D.M. Blake, 'Bibliography of Work on the Heterogeneous Photocatalytic Removal of Hazardous Compounds from Water and Air', National Renewable Energy Laboratory, NREL/TP-473-20300 (1995).
2. K. Rajeshwar, *J. Appl. Electrochem.* **25** (1995) 1067.
3. K. Rajeshwar and J. G. Ibanez, 'Environmental Electrochemistry' (Academic Press, New York, 1997), chapter 6.
4. G. Cooper and M.A. Ratcliff, 'Photocatalytic Treatment of Water', *US Patent 5 118 422* (2 June 1992).
5. R. Enzweiler, L. Wagg and J. Dong, American Institute of Chemical Engineers, Summer Meeting, Seattle, Washington, August (1993).
6. R.W. Matthews, *J. Chem. Soc., Faraday Trans. I* **85** (1989) 1291.
7. N.R. de Tacconi, J. Carmona and K. Rajeshwar, *J. Electrochem. Soc.* **144** (1997) 2486.
8. For example: J. Cunningham and P. Sedlak, *in* 'Photocatalytic Purification and Treatment of Water and Air', edited by D.F. Ollis and H. Al-Ekabi (Elsevier, Amsterdam, 1993), p. 67.
9. C.S. Turchi and E.J. Wolfrum, *J. Catal.* **136** (1992) 626.
10. K. Sopajaree, S.A. Qasim, S. Basak and K. Rajeshwar, *J. Appl. Electrochem.* (Part II, to be published).